Semnan University

Progress in Physics of Applied Materials

journal homepage: https://ppam.semnan.ac.ir/

Zn-MOF electrode material for supercapacitor applications

S. Salehi [1,*], M. Aghazadeh[1] , I. Karimzadeh[2]

[1]*Nuclear Fuel Research School, Nuclear Science and Technology Research Institute (NSTRI), Tehran, Iran*

[2]*Department of Physics, Faculty of Science, Central Tehran Branch, Islamic Azad University, Tehran, Iran*

ARTICLE INFO

Article history:
Received: 30 October 2022
Revised: 20 November 2022
Accepted: 21 November 2022

Keywords:
Electrodeposition; Energy storage and conversion; Metal-Organic-Frameworks; Specific capacitance

ABSTRACT

A Zn-based metal–organic framework (Zn-MOF) was synthesized by a novel electrodeposition method. The prepared Zn-MOF was characterized using powder X-ray diffraction, Fourier transform infrared spectroscopy, scanning electron microscopy (SEM) and energy dispersive X-ray spectroscopy techniques. The supercapacitive behavior of synthesized MOF was examined using cyclic voltammetry (CV), galvanostatic charge/discharge, and electrochemical impedance spectroscopy (EIS) measurements in 3 M KOH. SEM images confirmed that Zn-MOF is composed of layered cuboid structure properly attached on to nickel foam substrate. Electrochemical behaviors of the Zn-MOF/Ni foam were also evaluated through GCD tests, which showed high specific capacitance of 288 F g^{-1} at the current density of 2 A g^{-1}. The outcomes showed great potential of fabricated Zn-MOF as a high-performance electrode material for electrochemical supercapacitors.

1. Introduction

With the advancement of energy storage technology and the demand for renewable energy, supercapacitors as clean electrochemical energy storage devices are attracting attention because of their remarkable performance in storing energy [1]. High power density, satisfactory energy density and high rate cycle life are excellent features of supercapacitors [2]. Additionally, choosing proper active electrode materials can boost performance of supercapacitors.

Metal-organic-frameworks (MOFs) are class of active electrode materials which take advantage of the pseudocapacitance mechanism for storing energy [3]. MOFs are highly porous materials which are used as electrode active material lately. Their large surface areas, well distributed pore size and three dimensional structures as well as redox metal centers help storing charges [4]. In this regard, several studies have been applied the porous metal organic frameworks materials as electrode materials for supercapacitors applications. For example, Le et al. fabricated a Zn-MOF composite as supercapacitor materials. The prepared electrode showed specific capacitance of about 372 F/g in 1 M H_2SO_4 electrolyte at 1 A/g [5]. Hadise et al. synthesized cobalt terephthalate metal-organic framework (MOF-71) and applied it in energy storage devices which showed acceptable energy density of 13.51 Wh kg^{-1} [6]. Kishore et al. incorporated the Metal-organic framework (MOF-5) on NiCo2O4 and tested its electrochemical behavior. They prepared NiCo2O4/MOF-5 electrode exhibit a good specific capacitance of 357.69 F/g at 1 A/g [7].

Metal organic frameworks have been synthesized through different methods, such as solvothermal, hydrothermal, sonochemical, and chemical methods [8]. In storage applications, MOF materials are better to deposit on the electrode substrate directly to reduce the ohmic resistance and eliminate the binder [9]. Therefore, a binder-free electrodeposition technique provides some advantages over traditional methods like direct deposition of MOFs on the desired substrates, simple synthesisconditions, very short reaction times, low-cost approach, and easy to set-up [10].

Electrochemical synthesis process can be easily developed by a DC-power supply and a two-electrode set-up. By applying an optimized current density, the electrodepositing will be initialized. In this paper, we used reductive electrodeposition technique to synthesize Zn-MOF onto nickel foam and investigated its supercapacitive performance.

2. Experimental

2.1. Zn-MOF synthesis

In this procedure, zinc (II) nitrate hexahydrate [$Zn(NO_3)_2{\cdot}6H2O$] (1 mg) is dissolved in N,N-dimethyl-formamide [DMF] (15 mL) and well stirred for 20 minutes. Then 1 mg,

* Corresponding author. Tel.: +98-912-2312970
E-mail address: ***shiva.salehi10@gmail.com***

DOI: **10.22075/ppam.2022.28846.1036**

1,4 dicarboxybenzene [Terephthalic acid] was mixed with ethanol (15 mL) and stirred separately. Subsequently, the two solutions were mixed and stored for the deposition process.

Electrodepositing synthesis was run using a two-electrode set-up connected to a DC power supply. By applying a current density of 30 mA/cm^2 for 20 minutes the thin film of MOF was deposited on nickel cathodic substrate. The deposited nickel foam was removed from the solution and washed three times with DMF, and then it was kept for further analyses.

2.2. Material characterizations

The XRD patterns of MOF samples were tested by a PHILIPS/PW1730 with Cu-Ka radiation. Surface morphologies of the sample were obtained by scanning electron microscopy (SEM, Zeiss, with an applied potential of 30 kV). Using Scherrer equation the nano crystallite size (D) was calculated.

$$D = \frac{k\lambda}{\beta \cos\theta} \quad (1)$$

where λ is the XRD radiation wavelength, β is the full width at half maximum in radian and K is the shape factor which is about 0.89.

2.3. Electrochemical measurements

Electrochemical properties of the prepared electrode were investigated by a three-electrode electrochemical cell in 3 molar potassium hydroxide aqueous solution; the cell includes Zn-MOF/Ni foam (a working electrode), graphite plate (a counter electrode), and Ag/AgCl/saturated KCl (a reference electrode).

Cyclic voltammetry (CV), galvanostatic charge–discharge (GCD), and electrochemical impedance spectroscopy (EIS) measurements were run by potentiostat /galvanostat (Autolab). The EIS test was performed with the AC voltage of 10 mV amplitude and a frequency range of 0.01 Hz - 100 kHz. The mass loading of Zn-MOF onto nickel foam was 1 mg. CV profiles of the electrode were recorded within the potential window of 0 and 0.6 V vs. Ag/AgCl at the different scan rates of 5, 10, 20, 50, and 100 m V s^{-1}. The GCD tests were also performed at the current densities of 2, 3, 5, 10, 15, and 20 A g^{-1}. Helping the GCD data, the specific capacitances of the fabricated electrode were calculated by the following formula [11]:

$$C=(I \times \Delta t)/(m \times \Delta V) \quad (2)$$

In which, C in farad per gram is the measured capacitance, I in amper is the discharge current, Δt in second is the discharge time of electrode, ΔV in volt is the potential window, and m in gram is the mass of the loaded electrode active material.

3. Results and discussion

3.1. XRD

The XRD pattern of Zn-MOF/Ni foam is shown in Figure 1 the main diffraction peaks of fabricated electrode are in agreement with pattern of Zn-MOF reported in the literature [12]. The (100) crystal plane of Terephthalic acid -based MOF is recognized as the most intensive peak [13]. The sharp XRD peaks are observed at 44.10°, 51.8°, and 76.8° corresponding to the nickel foam. Thus, XRD studies proved the formation of Zn-MOF on to the nickel foam. Using Scherrer equation the crystallite size of MOF structure was calculated to be 2.97 nm.

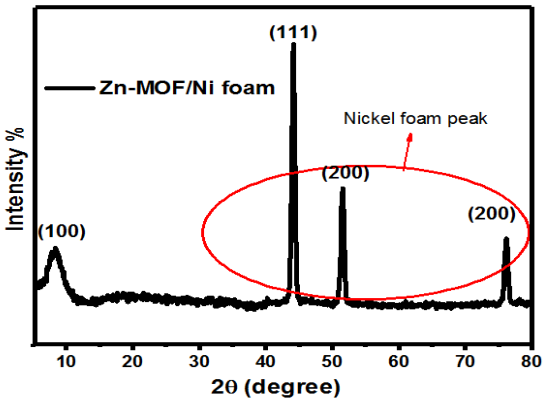

Fig. 1. XRD pattern of the fabricated Zn-MOF/Ni foam.

3.2. SEM

The morphology and composition of the as-prepared Zn-MOF/Ni foam are revealed by SEM at different magnification scales. At lower magnification the porous nickel foam is completely illustrated. According to the SEM images (Figure 2a, b), the Zn-MOF/Ni foam shows a layered cuboid structure with homogenous sizes distribution of about 1 μm width and 50 nm thickness.

This desired morphology could provide large contact area in the electrochemical reaction and shorten the electrolyte ion pathway [14].

3.3. Cyclic voltammetry tests

The electrochemical performance of Zn-MOF/Ni foam is studied by the three-electrode system in 3 M KOH aqueous electrolyte. Figure 3 illustrates CV curves of the fabricated Zn-MOF electrode at different scan rates from 5 to 100 mV s^{-1}. A pair of redox peaks is clearly seen on all CV curves, which reveals pseudocapacitive behavior of the Zn-MOF electrode [15].

These peaks may correspond to the intercalation and deintercalation of OH^- ion while electrochemical reactions are accrued. By increasing scanning rate, the current response is also gradually increased, showing excellent capacitive behavior and charge storage characteristics of the Zn-MOF electrode [16].

It can be easily observed that by increasing the scan rate, the anodic and cathodic peak potential shift toward positive and negative directions which indicate the ohmic resistance increase [17-19].

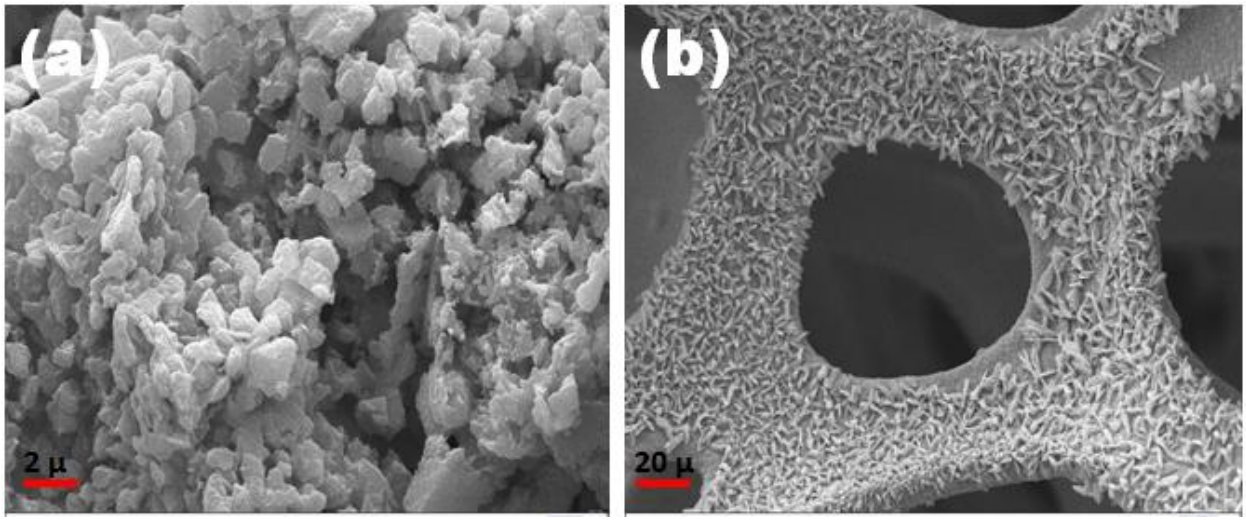

Fig. 2. SEM images of (a-b) Zn-BDC/Ni foam.

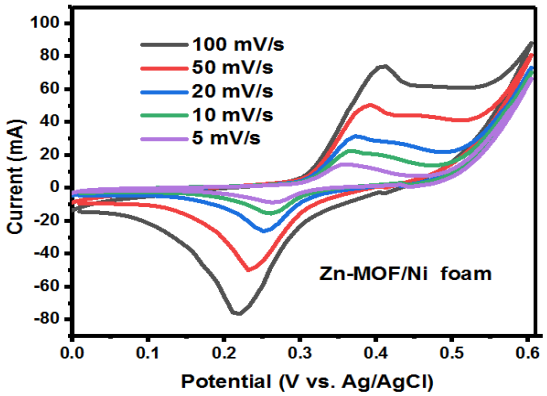

Fig. 3. Cyclic voltammetry curves of the Zn-BDC/Ni foams at the scan rate of 10, 20, 50, and 100 m V s^{-1}.

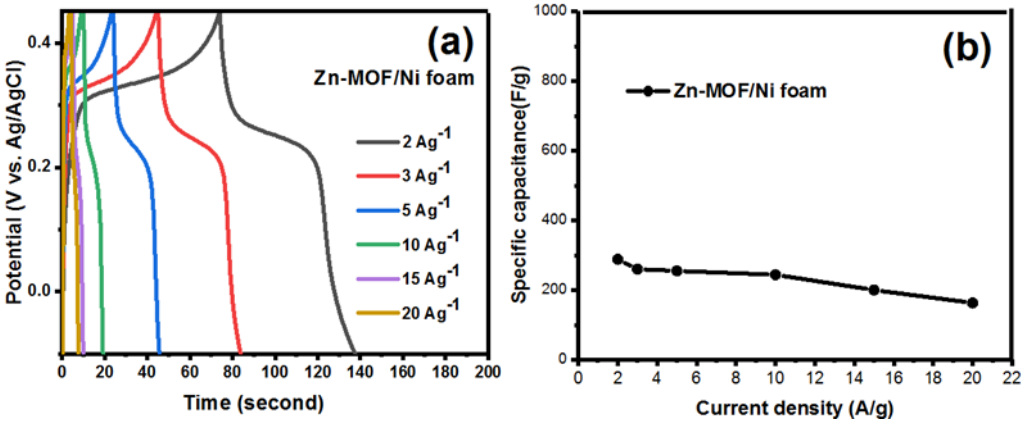

Fig. 4. (a) GCD curves of Zn-MOF/Ni foams at the current densities of 2, 3, 5, 10, 15, and 20 A g^{-1} and (b) the calculated specific capacitances at different current densities.

3.4. Galvanostatic Charge-Discharge tests

Fig. 4a shows the galvanostatic charge-discharge curves of the Zn-MOF electrode at different current densities in 3 M KOH solution within the potential window of 0 to 0.45 V.

From the GCD profile, the none linier response of the discharge curve exhibited pseudo-capacitive behavior of the electrode [16]. As it can be seen the longer duration time for charging–discharging belongs to the current density of 2 A g^{-1}, which showed the maximum specific capacitance of 288 F g^{-1}. The specific capacitances of the Zn-MOF/Ni foam electrode are calculated to be 288, 260, 255, 244, 200, and 163 F g^{-1} at the current densities of 2, 3, 5, 10, 15, and 20 A g^{-1}, respectively (Figure 4b). The capacitance retention of 56% is observed for the electrode.

Table 1. Some references for the capacitive data of the single metal MOF-based electrodes.

Electrode composition	Cs (F g^{-1})	Refs.
Co-MOF	220 at 1 A/g	[20]
Ni-MOF	849 at 1 A/g	[20]
Ni-MOF	164.37 at 1 A/g	[21]
Co-MOF/PANI	504 at 10 A/g	[22]
Fe-MOF	78 at 0.5 A/g	[23]
Co-MOF	206.76 at 1 A/g	[24]
Zn-MOF	221 at 1 A/g	[25]
Hu15 (Zn-MOF)	27.86 at 1 A/g	[26]
Zn-MOF/NF	288 at 1 A/g	This work

In Table 1, some capacitive data reported for MOF-based electrodes are listed from the literature. It was verified that our fabricated Zn-MOF electrode has shown great capacitive properties compared to electro-active materials in the other published literatures.

3.5. EIS

Electrical resistance of the fabricated electrode can be evaluated by electrochemical impedance spectroscopy (EIS) measurements. Figure 5 shows the Nyquist plot of the Zn-MOF/Ni foam electrode. The EIS test was examined in the frequency range of 0.01 Hz to 100 kHz at open circuit potential. The plot is composed of a semi-circle in the range of high frequency and a straight line in the range of low frequency. The semi-circle is related to Faradic reactions and showed charge transfer resistance (R_{ct}) [27]. The point intersection with the real impedance (Z') axis at the high frequency region implies the solution resistance (R_s) [28-31]. The calculated R_{ct} and R_s are 2.2 Ω and 1.5 Ω, respectively. Moreover, the equivalent circuit of the electrode was simulated by Zview software and the result is demonstrated in the inset image in Figure 5. Therefore, the prepared Zn-MOF electrode shows a good energy storage property for supercapacitor.

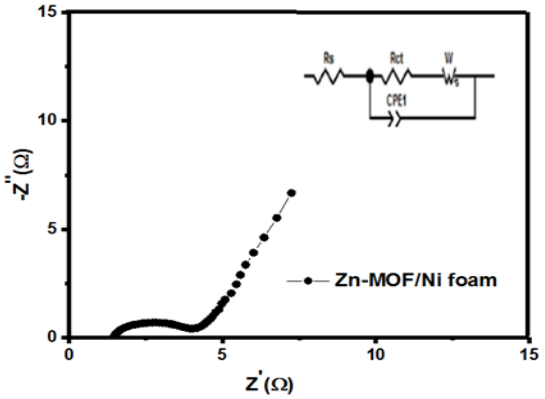

Fig. 5. Nyquist plot of Zn-MOF/Ni foam electrodes at the frequency range of 0.01 Hz to 100 kHz and its equivalent circuit.

4. Conclusion

In summary, a binder-free Zn-MOF/Ni foam electrode for energy storage aims was successfully synthesized by a facile electrochemical deposition method. The morphological characterization revealed the petal-like structures of Zn-MOF which were well attached on the surface of the nickel-foam. Electrochemical analyses were run a three electrode set-up in 3M potassium hydroxide media and the results demonstrated a pseudo-capacitive charge storage behavior of the fabricated electrode. The maximum specific capacitance of 288 F g^{-1} was delivered at the current density of 2 A g^{-1}.

Declaration of Competing Interest

The authors declare that they have no known competing financial interests or personal relationships that could have appeared to influence the work reported in this paper.

References

[1] S. Hussain, A.J. Khan, M. Arshad, M.S. Javed, A. Ahmad, S.S. Ahmad Shah, M.R. Khan, S. Akram, S. Ali, Z.A. ALOthman, G. Liu, "Charge storage in binder-free 2D-hexagonal CoMoO4 nanosheets as a redox active material for pseudocapacitors." Ceramics International 47 (2021), 8659–8667.

[2] B. Asbani, G. Buvat, J. Freixas, M. Huvé, D. Troadec, P. Roussel, T. Brousse, C. Lethien, "Ultra-high areal capacitance and high rate capability RuO2 thin film electrodes for 3D micro-supercapacitors." Energy Storage Materials 42 (2021) 259–267.

[3] Y. Peng, J. Xu, J. Ma, Y. Bai, S. Cao, S. Zhang, H. Pang, "Metal-organic framework (MOF) composites as promising materials for energy storage applications." Advances in Colloid and Interface Science 307 (2022) 102732.

[4] S. Kavian, S. Hajati, M. Moradi, "High-rate supercapacitor based on NiCo-MOF-derived porous NiCoP for efficient energy storage." Journal of Materials Science: Materials in Electronics 32 (2021) 13117–13128.

[5] T. H. Nguyen, H. Fei, I. Sapurina, F.A. Ngwabebhoh, C. Bubulinca, L. Munster, E. D. Bergerová, A. Lengalova, A. H. Jiang, T.T. Dao, N. Bugarova, "Electrochemical performance of composites made of rGO with Zn-MOF and PANI as electrodes for supercapacitors." Electrochimica Acta 367 (2021) 137563.

[6] H. Bigdeli, M. Moradi, S. Hajati, M. A. Kiani, J. Toth, "Cobalt terephthalate MOF-templated synthesis of porous nano-crystalline Co3O4 by the new indirect solid state thermolysis as cathode material of asymmetric supercapacitor." Physica E: Low-Dimensional Systems and Nanostructures 94 (2017) 158–166.

[7] M. Jayachandran, T. Maiyalagan, T. Vijayakumar, B. Gunasekaran, "Metal-organic framework (MOF-5) incorporated on NiCo2O4 as electrode material for supercapacitor application." Materials Letters 302 (2021) 130338.

[8] B. Abdollahi, S. Farshnama, E. Abbasi Asl, A. Najafidoust, M. Sarani, "Cu(BDC) metal–organic framework (MOF)-based Ag2CrO4 heterostructure with enhanced solar-light degradation of organic dyes." Inorganic Chemistry Communications 138 (2022) 109236.

[9] M. V. Varsha, G. Nageswaran, "Direct Electrochemical Synthesis of Metal Organic Frameworks." Journal of The Electrochemical Society 167 (2020) 155527.

[10] A. Ghoorchian, A. Afkhami, T. Madrakian, M. Ahmadi, "Electrochemical synthesis of MOFs." Metal-Organic Frameworks for Biomedical Applications (2020). 177–195.

[11] M. Aghazadeh, I. Karimzadeh, M. R. Ganjali, "Preparation of Nano-sized Bismuth-Doped Fe3O4 as an Excellent Magnetic Material for Supercapacitor Electrodes." Journal of Electronic Materials *47* (2018) 3026–3036.

[12] M. Yang, Q. Bai, "Flower-like hierarchical Ni-Zn MOF microspheres: Efficient adsorbents for dye removal." Colloids and Surfaces A: Physicochemical and Engineering Aspects 582(2019) 123795.

[13] J. Yang, , P. Xiong, C. Zheng, H. Qiu, M. Wei, "Metal-organic frameworks: A new promising class of materials for a high performance supercapacitor electrode." Journal of Materials Chemistry A 2(2014) 16640–16644.

[14] F. Cao, M. Gan, , L. Ma, , X. Li, , F. Yan, M. Ye, Y. Zhai, Y. Zhou, "Hierarchical sheet-like Ni–Co layered double hydroxide derived from a MOF template for high-performance supercapacitors." Synthetic Metals 234(2017) 154–160.

[15] G. J. H. Lim, X. Liu, C. Guan, J. Wang, "Co/Zn bimetallic oxides derived from metal organic frameworks for high performance electrochemical energy storage." Electrochimica Acta 291(2018) 177–187.

[16] Y. Jiao, J. Pei, D. Chen, C. Yan, Y. Hu, Q. Zhang, G. "Chen, Mixed-metallic MOF based electrode materials for high performance hybrid supercapacitors." Journal of Materials Chemistry A 5 (2017) 1094–1102.

[17] H. Liang, R. Liu, C. Hu, X. An, X. Zhang, H. Liu, J. Qu, "Synergistic effect of dual sites on bimetal-organic frameworks for highly efficient peroxide activation." Journal of Hazardous Materials 406 (2021) 124692.

[18] Q. Zha, F.Yuan, G.Qin, Y. Ni, "Cobalt-Based MOF-on-MOF Two-Dimensional Heterojunction Nanostructures for Enhanced Oxygen Evolution Reaction Electrocatalytic Activity." Inorganic Chemistry 59(2020) 1295–1305.

[19] Y. Li, M. Xie, X. Zhang, Q. Liu, D. Lin, C. Xu, F. Xie, X. Sun, "Co-MOF nanosheet array: A high-performance electrochemical sensor for non-enzymatic glucose detection." Sensors and Actuators B: Chemical 278(2019) 126–132.

[20] M.S. Rahmanifar, H. Hesari, A. Noori, M.Y. Masoomi, A. Morsali, M.F. Mousavi, "A dual Ni/Co-MOF-reduced graphene oxide nanocomposite as a high performance supercapacitor electrode material." Electrochimica Acta, 275 (2018) 76–86.

[21] X. Li, J. Li, Y. Zhang, P. Zhao, "Synthesis of Ni-MOF derived NiO/rGO composites as novel electrode materials for high performance supercapacitors." Colloids and Surfaces A: Physicochemical and Engineering Aspects 622(2021) 126653.

[22] R. Srinivasan, E. Elaiyappillai, E.J. Nixon, I. Sharmila Lydia, P.M. Johnson, "Enhanced electrochemical behaviour of Co-MOF/PANI composite electrode for supercapacitors." Inorganica Chimica Acta 502 (2020) 119393.

[23] H. Yu, H. Xia, J. Zhang, J.He, S. Guo, Q. Xu, "Fabrication of Fe-doped Co-MOF with mesoporous structure for the optimization of supercapacitor performances." Chinese Chemical Letters 29 (2018) 834–836.

[24] D.Y. Lee, S.J. Yoon, N.K. Shrestha, S.H. Lee, H. Ahn, S.H. Han, "Unusual energy storage and charge retention in Co-based metal-organic-frameworks." Microporous and Mesoporous Materials 153(2012) 163–165.

[25] S. Umezawa, T. Douura, K. Yoshikawa, D. Tanaka, V. Stolojan, S.R.P. Silva, M. Yoneda, K. Gotoh, Y. Hayashi, "Zinc-Based Metal–Organic Frameworks for High-Performance Supercapacitor Electrodes: Mechanism Underlying Pore Generation." Energy and Environmental Materials (2022).

[26] H. He, G. Wang, B. Shen, Y. Wang, Z. Lu, S. Guo, J. Zhang, L. Yang, Q. Jiang, Z. Xiao, "Three isostructural Zn/Ni nitro-containing metal-organic frameworks for supercapacitor." Journal of Solid State Chemistry 288 (2020) 121375.

[27] B.Y. Chang, S.M. Park, "Electrochemical impedance spectroscopy. "Annual Review of Analytical Chemistry, 3(2010) 207–229.

[28] N.O. Laschuk, E. Bradley Easton, O.V. Zenkina, "Reducing the resistance for the use of electrochemical impedance spectroscopy analysis in materials chemistry" RSC advances 11 (2012) 27925-36.

[29] P. Vadhva, J. Hu, M.J. Johnson, R. Stocker, M. Braglia, D.J.L. Brett, A.J.E. Rettie, "Electrochemical Impedance Spectroscopy for All-Solid-State Batteries: Theory, Methods and Future Outlook." In ChemElectroChem 8 (2021) 1930–1947.

[30] S. Salehi, M.H. Ehsani, M. Aghazadeh, A. Badiei, M.R. Ganjali, "Electrodeposition of binderless Ni,Zn-MOF on porous nickel substrate for high-efficiency supercapacitors." Journal of Solid State Chemistry 316(2022) 123549.

[31] M.R. Pallavolu, A.N. Banerjee, R.R. Nallapureddy, S.W. Joo, "Urea-assisted hydrothermal synthesis of MnMoO4/MnCO3 hybrid electrochemical electrode and fabrication of high-performance asymmetric supercapacitor." Journal of Materials Science and Technology 96(2022) 332–344.